Chapter 1
LEAP-UCD-2017 V. 1.01 Model Specifications

Bruce L. Kutter, Trevor J. Carey, Nicholas Stone, Masoud Hajialilue Bonab, Majid T. Manzari, Mourad Zeghal, Sandra Escoffier, Stuart K. Haigh, Gopal S. P. Madabhushi, Wen-Yi Hung, Dong-Soo Kim, Nam Ryong Kim, Mitsu Okamura, Tetsuo Tobita, Kyohei Ueda, and Yan-Guo Zhou

B. L. Kutter (✉) · T. J. Carey · N. Stone
Department of Civil and Environmental Engineering, University of California, Davis, CA, USA
e-mail: blkutter@ucdavis.edu

M. H. Bonab
Department of Civil Engineering, University of Tabriz, Tabriz, Iran

M. T. Manzari
Department of Civil and Environmental Engineering, George Washington University, Washington, DC, USA

M. Zeghal
Department of Civil and Environmental Engineering, Rensselaer Polytechnic Institute, Troy, NY, USA

S. Escoffier
IFSTTAR, GERS, SV, Bouguenais, France

S. K. Haigh · G. S. P. Madabhushi
Department of Engineering, Cambridge University, Cambridge, UK

W.-Y. Hung
Department of Civil Engineering, National Central University, Jhongli City, Taoyuan, Taiwan

D.-S. Kim
Department of Civil and Environmental Engineering, Korea Advanced Institute of Science and Technology, Yuseong, South Korea

N. R. Kim
K-water Research Institute, Korea Water Resources Corporation, Daejeon, South Korea

M. Okamura
Department of Civil Engineering, Ehime University, Matsuyama, Japan

T. Tobita
Department of Civil Engineering, Kansai University, Osaka, Japan

K. Ueda
Disaster Prevention Research Institute, Kyoto University, Kyoto, Japan

Y.-G. Zhou
Department of Civil Engineering, Zhejiang University, Hangzhou, China

B. Kutter et al. (eds.), *Model Tests and Numerical Simulations of Liquefaction and Lateral Spreading*, https://doi.org/10.1007/978-3-030-22818-7_1

Abstract This paper describes the specifications developed by and distributed to all of the centrifuge test facilities involved in LEAP-UCD-2017. The specified experiment consisted of a submerged medium dense clean sand with a 5-degree slope subjected to 1 Hz ramped sine wave base motion in a rigid container. This document describes the detailed geometry, sensor locations, methods of preparation, quality control, shaking motions, surface markers, and surface survey techniques.

1.1 Introduction

1.1.1 Differences Between This Paper and Pre-test Specifications

This paper documents the specifications for LEAP-UCD-2017 centrifuge model tests as they existed just prior to the testing for LEAP-UCD-2017. The primary goal of the specifications was to improve the specimen preparation, the testing procedures, and the accuracy of the data and in addition to provide data to quantify the uncertainties associated with the experiments. The specifications were first drafted for the LEAP-GWU-2015 project described by Kutter et al. (2017). Based upon experience in 2014–2015, the specifications were updated and improved for the LEAP-UCD-2017 exercise.

While some of the data in this paper (e.g., the maximum and minimum densities) were subsequently superseded, it was decided to maintain this document as it was prior to centrifuge testing as a record of the specifications. The remainder of this paper is therefore nearly a verbatim copy the specifications developed prior to the centrifuge testing.

1.1.2 Goals and Overview

The goals of this LEAP are to perform a sufficient number of experiments to characterize the median response and the uncertainty of the median response of a specific sloping deposit of sand to a specified ground motion. To put the uncertainty in context, it was considered critical to also determine the sensitivity of response to relative density, the sensitivity of the response to the ground motion intensity, and the sensitivity of the response to unspecified components of the ground motion that are superimposed on the specified ground motion.

The specific median soil deposit to be tested at each centrifuge facility is a 4-m-deep, 20-m-long deposit of Ottawa F-65 sand with a dry density of about 1650 kg/m^3 and a ground slope of 5°. The specified median ground motion is a ramped sine wave input motion similar to the target motion for LEAP-GWU-2015. The primary response quantity of interest is the displacement and deformed shape of the soil deposit. Important secondary response quantities include time series data from acceleration, pore pressure, and displacement sensors.

1.2 Scaling Laws

The length scale factor, L^*, is defined as $L^* = L_{model}/L_{prototype}$. According to the conventional centrifuge scaling laws, gravity will be scaled according to $g^* = 1/L^*$. The gravity in the model $g_{model} = \omega^2 R_{ref}$, where R_{ref} is measured at 1/3 the depth of sand in the middle of the plan area of the soil deposit. Viscous pore fluid will be used in all the experiments and the viscosity should be scaled according to $\mu = \mu_{water}/L^*$. Scaling laws are used in accordance with recommendations by Garnier et al. (2007).

1.3 Description of the Model Construction and Instrumentation

1.3.1 Soil Material: Ottawa F-65 Sand

Ottawa F-65 sand was chosen as the standard sand for LEAP-GWU-2015 and LEAP-UCD-2017. Ottawa F-65 sand is a clean (less than 0.5% fines), sub-rounded to sub-angular whole grain silica sand, provided by US Silica, in Ottawa, Illinois. Specific gravity and grain size parameters determined during LEAP-GWU-2015 are summarized in Table 1.1; results from maximum and minimum dry density tests are given in Table 1.2. Additional material properties of Ottawa F-65 sand, including triaxial, simple shear, and permeability test data, may be found in the LEAP Soil Properties and Element Test Database (Carey et al. 2017).

It appears from standard deviations given in Table 1.1 that the grain sizes of the tested sand were very consistent. (It should be noted that many sites used 0.25 and 0.125 mm sieve sizes without intermediate sieve sizes, so the values of D_{10}–D_{60} were interpolated between the percentages retained on those two sieves; this interpolation is estimated to produce errors on the order of 0.01 mm for D_{30} and D_{50}.)

In late 2016, however, a different batch of sand delivered from US Silica to UC Davis had quite different grain sizes; D_{50} was approximately 0.28 mm and some variability was noticed from bag to bag. The 2016 batch of material was considered

Table 1.1 Specific gravity and grain size characteristics of Ottawa F-65 sand used in LEAP-GWU-2017 (Kutter et al. 2017)

	Num of Tests	Average	Stand. Dev.
G_s	4	2.665	0.012
D_{10} (mm)	5	0.133	0.005
D_{30} (mm)	5	0.173	0.009
D_{50} (mm)	5	0.203	0.013
D_{60} (mm)	5	0.215	0.016
Fines (%)	5	0.154	0.133

Table 1.2 Maximum and minimum dry density for Ottawa F-65 sand (Kutter et al. 2017)

Data source	Test method	Min. density (kg/m^3)	Max. density (kg/m^3)
Cooper Labs (UCD)	ASTM D4254 and D4253	1515	1736
GeoTesting Express (RPI)	ASTM D4254 and D4253	1494	1758
Andrew Vasco (GWU)	ASTM D4254 and D4253	1538	1793
Andrew Vasco (GWU)	Lade et al. (1998)(using graduated cylinder)	1521	1774
Cerna Alvarez (UCD)	Lade et al. (1998) (using graduated cylinder)	1415	1720
Cerna Alvarez (UCD)	Modified ASTM D4254(a)	1406	
Parra Bastidas (UCD)	ASTM D4254, JIS A 1224	1455	1759
Wen-Yi Hung (NCU)	—	1482	1781
Yan-Guo Zhou (ZJU)	DL/T5355-2006[a]	1456	1733
Average of tests		1475	1756
Stand. dev. of all methods		46	25

Please see Carey et al. paper in this proceedings describing more recent index density tests
[a]Chinese "Code for soil tests for hydropower and water conservancy engineering," 2006

to be non-satisfactory for LEAP. All of the sand shipped from Davis in early 2017 to LEAP participants was therefore taken from the original batch of sand shipped to UC Davis in 2014. Unfortunately, the inconsistency in the later delivery has raised concerns about the quality control of the sand in the future. Therefore, it is important for each LEAP site to perform quality control checks on the grain characteristics of the Ottawa F-65 sand. A sufficient number of bags to prepare an entire model should be mixed together first, and then the grain size analysis and maximum and minimum tests should be conducted on this mixture. If the grain size is significantly different from that in Table 1.1, researchers should scalp the material so that D_{50} and D_{10} conform to be within one standard deviation of the data reported in Table 1.1. In addition, at least one maximum and minimum density test, as described below, should be performed on the mixed material used for each centrifuge model.

The sand placement is to be prescribed based on a target density (as opposed to relative density) to avoid the small conversion error associated with uncertainty in specific gravity and larger uncertainty associated with maximum and minimum densities. From Table 1.3, it can be seen that considerable scatter is observed in the values of maximum and minimum density. The two experiments performed by professional laboratories in the USA according to ASTM D4253 and D4254 were quite consistent with each other. But use of a 1000 ml graduated cylinder (modified Lade et al. approach) typically produced significantly lower minimum densities.

$$D_r = \frac{\rho_{d\max}(\rho_d - \rho_{d\min})}{\rho_d(\rho_{d\max} - \rho_{d\min})} \tag{1.1}$$

Table 1.3 Grain size parameters of Ottawa F-65 sand published by US Silica

USA STD SIEVE SIZE		TYPICAL VALUES % RETAINED		% PASSING
MESH	MILLIMETERS	INDIVIDUAL	CUMULATIVE	CUMULATIVE
30	0.600	0.0	0.0	100.0
40	0.425	0.1	0.1	99.9
50	0.300	4.0	4.1	95.9
70	0.212	37.0	41.1	58.9
100	0.150	45.8	86.9	13.1
140	0.106	11.4	98.3	1.7
200	0.075	1.6	99.9	0.1
270	0.053	0.1	100.0	0.0

To facilitate frequent quality control, a simple and consistent method of measuring maximum and minimum densities is required. Researchers are requested to measure maximum and minimum densities at least once for each model test. The methods described below should be used (modified from ASTM procedures). In addition, researchers may decide to measure the index densities using common standard procedures used in their country. A new section of the data reporting template for reporting the results of the grain size and maximum/minimum densities will be developed soon.

Independent measurement of any of the soil properties should be reported using a spreadsheet with format consistent with the formats of existing soil properties in the LEAP Soil Properties and Element Test Database (https://nees.org/resources/13689/).

Modified ASTM D4254 Method C for Minimum Dry Density

A glass graduated cylinder of 1000 ml will be used for measurement of the minimum density. The humidity of the "dry" sand source should be measured by burying a humidity sensor into the sand until the reading stabilizes. The humidity of the room should also be measured. About 500 g of dry sand should be carefully weighed and placed inside a 1000 ml graduated cylinder. The top of the graduated cylinder should be covered with a sheet of latex and held by hand to seal the top of the cylinder. The sample should then be turned upside down and steadily rotated upright within about 60 s. The volume of the loose sample can then read from the graduated cylinder. Data to be recorded include date, researcher, mass of sand, volume of loose sand, humidity of the laboratory, humidity of the sand source, temperature of the room, and the minimum dry density. The calibration of the volume marks on the side of the graduated cylinder should be checked by weighing it with a known volume of water and assuming the density of water is 998 kg/m^3.

Modified Lade et al. (1998) Method for Maximum Density

Place approximately 500 g of soil in approximately 50 g increments into a plastic 1000 ml graduated cylinder. After placing each 50 g increment, the side of the graduated cylinder should be firmly tapped eight times (two times each on the north, south, east, and west sides of the cylinder) with the plastic handle of a screwdriver. The mass of the screwdriver should be approximately 140 g and total length of about 250 mm. To consistently apply the firm taps, the operator should hold the screwdriver by the metal part, and the plastic handle should be about 250–300 mm away from the cylinder between taps to produce consistency. After the last 50 g increment of soil is placed and tapped, each of four sides of the graduated cylinder should be lightly tapped six times (24 total) up and down the sample. To level the top surface for purposes of accurate reading, five or ten very light taps are made while the cylinder is tilted. The volume of the sand may be read from the graduated cylinder and the maximum density calculated. Data to be recorded include date, researcher, mass of sand, volume of loose sand, humidity of the laboratory, humidity of the sand source, temperature of the room, and the maximum density. A video of the recommended procedure for checking maximum and minimum density is posted in the General Report for the data archive for LEAP-UCD-2017 (https://doi.org/10.17603/DS2N10S).

1.3.2 Placement of the Sand by Pluviation

The sand should be pluviated through a screen with opening size approximately 1.20 mm. The screen will be partially blocked to restrict the flow (see Fig. 1.1). Three arrangements with different parts of the screen masked off should be used to achieve different sample densities as indicated in Fig. 1.2. Small modifications to the opening patterns are allowable if necessary. In the tests used to create Fig. 1.3, 100-mm-long slots in a US standard sieve were used. If the screens need to be placed inside the model container during pluviation, a non-circular sieve may be fabricated to facilitate pouring near the edges and corner of the container. The 1.2 mm screen may be cut from a standard sieve, and the screen may be placed in a rectangular-shaped custom sieve. To avoid cutting a good sieve, the screen may be available from rolls from soil mechanics laboratory suppliers. The slot lengths in a rectangular screen should be greater than or equal to 100 mm.

If the screen or the geometry of the open parts of the screen is significantly modified, calibration curve (density as a function of drop height), mass flow rate during deposition, as well as the dimensions of the container used to perform the calibration will be reported in the data report.

The elevation of the screen above the container during pluviation should be continually adjusted to maintain a constant vertical spacing between the sand surface and the screen; the drop height should not change by more than 5% during

Fig. 1.1 (**a**) Standard sieve used for calibration tests in this specification. (**b**) Side view of sand falling for 7.1 mm slots spaced at 17 mm. (**c**) Duct tape used to mask off slots for pluviation; the 7.1 mm slots correspond to three mesh widths of the standard sieve. (**d**) Ad hoc arrangement of sieve attached to hopper used to feed sand to the sieve during pluviation

deposition. The sieve should be steadily and continuously moved (by robot or by hand) to avoid local mounds with side slopes that affect the deposition. Some tapping of the sieve is necessary if/when the sieves become clogged.

Calibration curves for the above three screen masking patterns are presented in Fig. 1.3. If researchers notice a significant difference in the calibration curve, they should report their observed calibration curve (density vs drop height).

It is suspected that humidity of the sand and electrostatic forces developed during repeated handling of the sand could affect the results. To investigate these issues, a sideview photograph of the sand flowing should be included in the sample preparation report. A humidity sensor should be embedded into the sand after deposition to measure the temperature and humidity of the sand after placement. The humidity of the room should also be measured. Suitable humidity sensors, for example, are

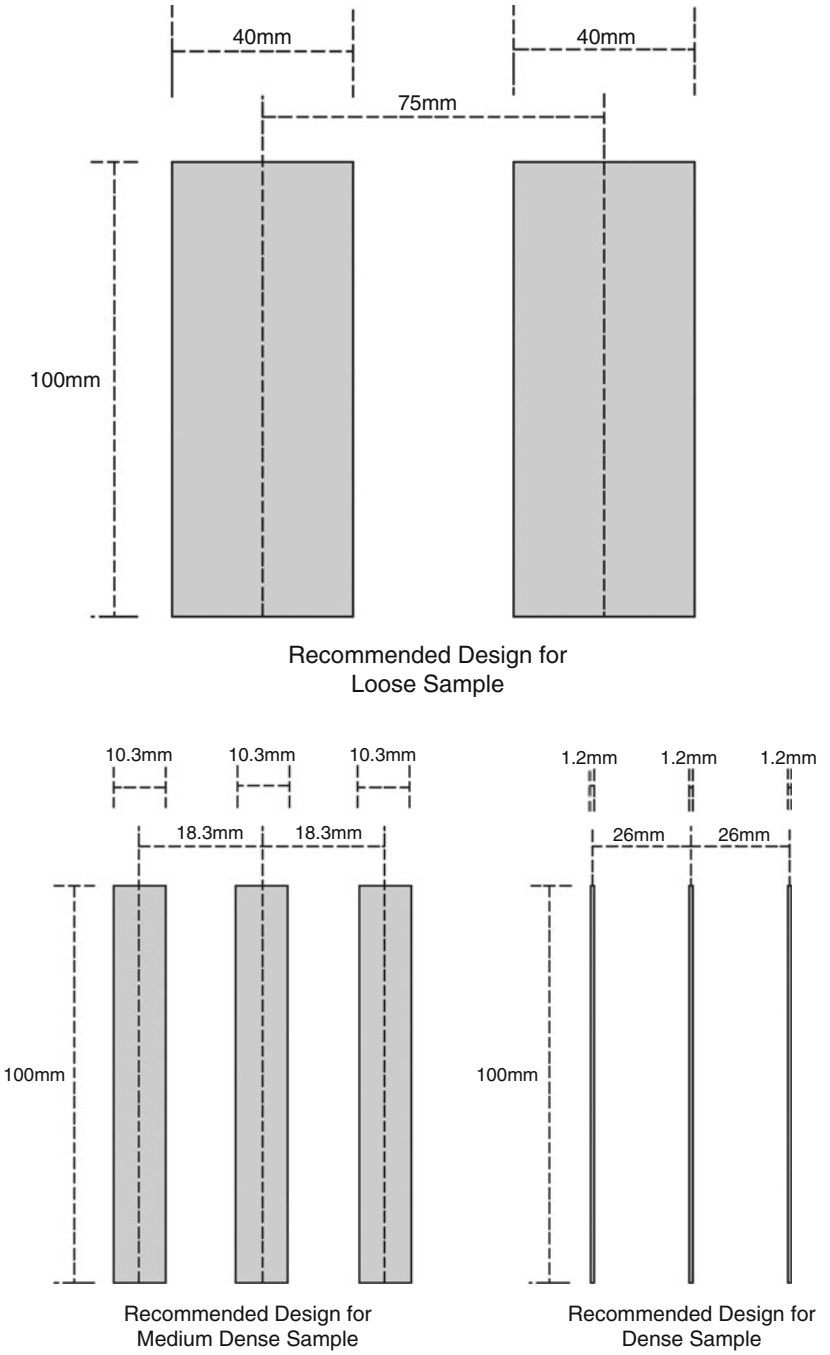

Fig. 1.2 Recommended opening dimensions to be masked off over a mesh of 1.18–1.22 mm opening to achieve different densities of samples by dry pluviation. The mass flow rates for these designs were 3.6, 2.5, and 1 kg/min with flow rates increasing as slot width increases

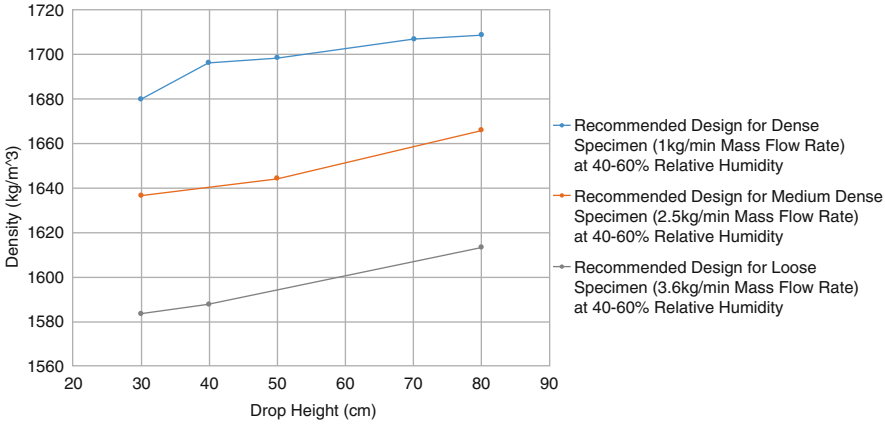

Fig. 1.3 Density vs drop height (from tests at UCD in Jan to March 2017) for three recommended sieve designs tested at 40–60% relative humidity. The blue, red, and black lines correspond to the slot dimensions shown in Fig. 1.2

available in the USA for approximately $75 (http://www.testequipmentdepot.com/extech/pdf/rh300.pdf).

1.3.3 Measurement of Density of the Sand

To measure the as-deposited density of the sand in the model container, an accurate method of measuring the container dimensions and the volume of the sand in the container is required. Container dimensions may be measured accurately using a rigid steel ruler and then the volume of the container checked by filling the container with water, covering it with a flat plate, eliminating air bubbles, and measuring the mass of water that it holds. Confirm that the volumes computed from dimensions and water mass are consistent; check and report their repeatability.

A suggested method for measuring the sand height is to smooth the surface of the sand using a 25-mm-thick, approximately 70-mm-diameter, acrylic plastic disk as shown in Fig. 1.4 followed by placement of about 15 or more 20-mm-diameter, 6-mm-thick PVC or HDPE disks gently on the surface as uniformly spaced representative grid locations. The disks may be lightly twisted without pushing down to make their base rest evenly on the sand. Using a Vernier caliper, measure the location of the disks relative to a stiff smooth beam across the top of the model container as indicated in Fig. 1.4c. The average height of the sand must be determined to an accuracy better than 0.5%. Superior tools for measuring volume are acceptable if the process and accuracy are documented.

The mass of the sand should also be measured to better than 0.5%. The accuracy and the repeatability of the measuring method should be verified.

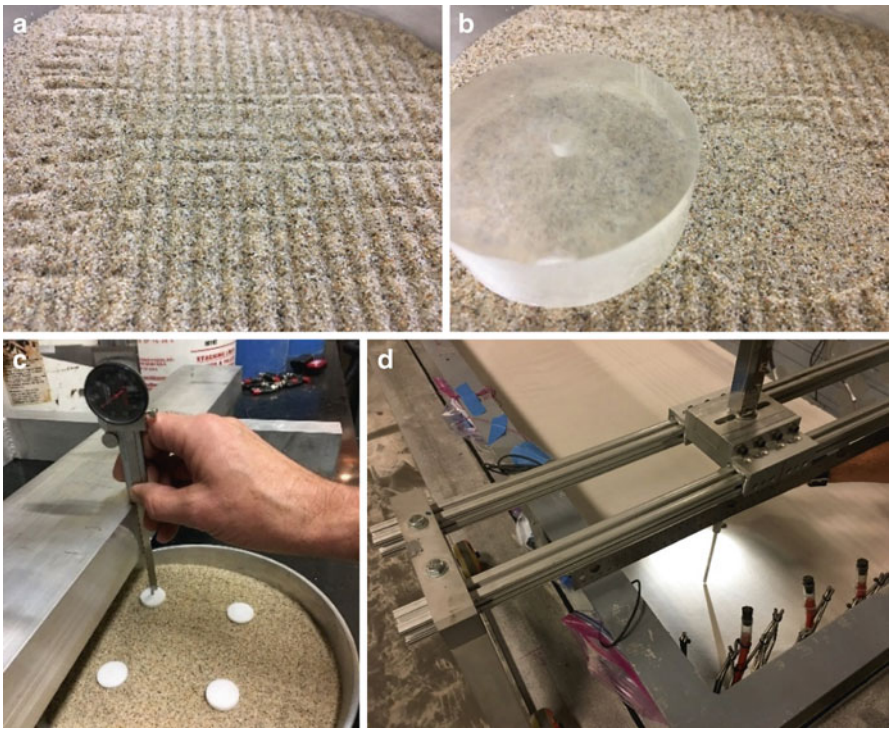

Fig. 1.4 Illustration of recommended method to measure the volume of sand specimen. (**a**) Rough surface of sand after shaping with vacuum. (**b**) 25 × 70 mm acrylic disk lightly set down on surface, slightly twisted as necessary to smooth the surface. (**c**) 5-mm-thick × 18-mm-diameter PVC or HDPE plastic disks gently placed on the smoothed sand in a grid. X, Y, and Z coordinates of the disk to be measured using caliper. (**d**) Measuring rails used on the large centrifuge at UCD. Good quality of light with a distinct shadow aids in resolving the location of the surface

1.3.4 Geometry of the Model

The required shape of soil surface depends on direction of shaking relative to the curved g-field as shown in Fig. 1.5. In addition, if the centrifuge bucket is not freely swinging (e.g., for the Cambridge centrifuge where the bucket swing seats against stops), then the surface of the sand should be modified to eliminate unintended slope angles in any direction.

1.3.5 Saturation of the Model

To facilitate dissolution of gas bubbles that are trapped in the sand, the model container will be repeatedly evacuated and flooded with CO_2 to replace 98% of

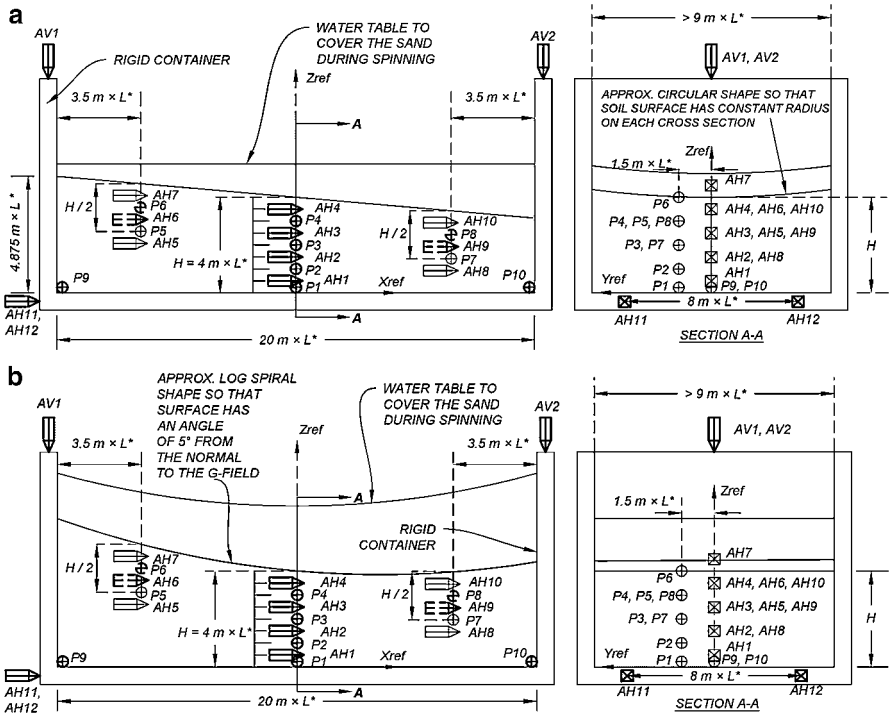

Fig. 1.5 (**a**) Baseline schematic for LEAP-UCD-2017 experiment for shaking parallel to the axis of the centrifuge. Bold sensors are required. Bold-dashed sensors are highly recommended. Thin-lined sensors are recommended. (**b**) Baseline schematic for LEAP-UCD-2017 experiment for shaking in the circumferential direction of the centrifuge. Bold sensors are required. Bold-dashed sensors are highly recommended. Thin-lined sensors are recommended

the air in the chamber by pure CO_2 prior to saturation with de-aired viscous fluid (Kutter 2013). If 90% vacuum is applied, then the process must be repeated at least twice to remove more than 98% of the air. If 50% vacuum is applied, then the vacuum and CO_2 flooding should be repeated at least five times. After 98% replacement of air by CO_2, de-aired viscous pore fluid should be dripped into the low end of the model slope followed by infiltration with de-aired water while under vacuum as shown in Fig. 1.6. The de-aired viscous fluid may be prepared by letting it sit under a vacuum of at least 80 kPa (absolute pressure is 21 kPa or less). The vacuum should be continuously applied to the water supply reservoir while it is being introduced to the specimen. If this is not possible, steps should be taken to prevent gas from re-dissolving in the fluid prior to infiltration. Flow of viscous fluid to the model from the reservoir may be driven by gravity feed or peristaltic pump.

Documentation that the method of saturation is successful either by the measurement of p-wave velocity or by measuring the raising and lowering of the water level due to applying vacuum to the entire container (as described by Okamura and Inoue 2012) is required.

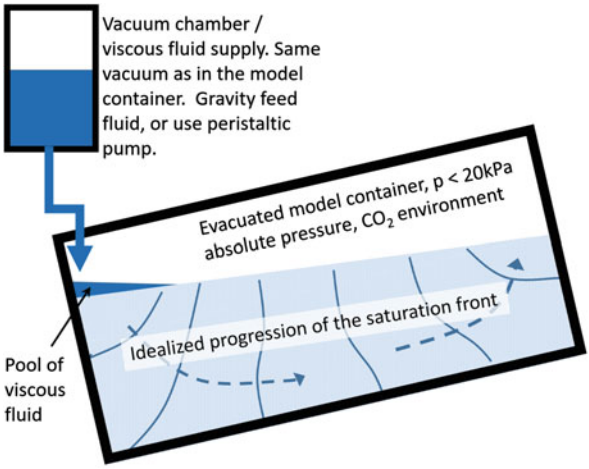

Fig. 1.6 Saturation by dripping de-aired viscous fluid under vacuum into the container. Once a pool has formed at the low end of the soil surface, the pool should be continuously maintained with some free pore fluid. The elevation of the pool may gradually be increased to cover the outcrop of the saturation front. A sponge may be placed on the surface of the sand to protect the sand from the impact of fluid dropping from the vacuum chamber. The tilting of the box by a few degrees is suggested to help reduce likelihood of trapping an air pocket in the bottom corner of the box

1.4 Instrumentation of the Model

1.4.1 Required Instrumentation

The required instrumentation is very similar to that for LEAP-GWU-2015 as indicated in Fig. 1.5a, b. AH1–AH4, AH11, AH12, AV1, AV2, P1–4, P9, and P10 are required sensors. AH6, AH9, P6, and P8 are highly recommended. AH5, AH7, AH8, AH10, P5, and P7 are recommended sensors. Bender elements are also recommended be used to monitor the evolution of the shear wave velocity during the centrifuge testing. To the extent possible, cables from the sensors should run in the transverse direction toward the side walls of the model container to minimize the reinforcing effect of the sensor cables. The routing of cables should avoid regions were CPT tests could intersect the cables.

1.4.2 Displacement Measurements

As described by Kutter et al. (2017), it is possible to determine dynamic displacements by integration of accelerometer records. Acceleration records should therefore be reported with as little analog and digital signal processing as possible; if filtering is necessary, the characteristics of the filter must be indicated. The corner frequencies of the data acquisition system should be reported, especially for the accelerometer sensors.

There is clearly a fundamental difficulty associated with measuring residual or permanent displacements from contact sensors founded in submerged liquefied, laterally spreading ground. A concerted effort is required to obtain more accurate displacement measurements than has been achieved in the past.

At least four techniques to be pursued for determining displacements are described below. Experimenters are encouraged to share innovations that will enable improved displacement measurements. If it is not possible to assess lateral displacements before and after shaking from the cameras or pore pressure sensors, then some alternate method such as an LVDT, linear potentiometer, or laser displacement sensor should be used to determine lateral and vertical displacements as accurately as possible.

Careful Before and After Photographs of the Model and Surface Markers

Prior to spinning the centrifuge, after stopping after the first destructive motion, and after all of the destructive shaking events, photographs must be taken. The photographs should use a camera looking vertically down at the center of the specimen at the same distance and in the same lighting conditions. The location of the camera should be carefully placed above the top center of the model, and good lighting should be used to enable these reference photos to be used to determine the lateral deformation at various stages of the testing. These reference photographs should be taken using the same camera, with the same lens with the same amount of water on top of the specimen and with similar lighting. Make sure that the surface markers are clearly visible in the photographs.

Surface markers can be manufactured by 3D printing. The images in Fig. 1.7 are from an order placed by UCD. The shape of the markers is designed to anchor to the soil and provide minimal restriction to pore pressure drainage, with a taper to facilitate insertion with reduced disturbance. The sand in the middle of the markers may also be colored to improve edge contrast for image analysis of marker locations. The markers were made from a plastic material with specific gravity of approximately 1.5. The file used to produce the markers, Surface_Marker_ImprovedDesign.stl, is in an industry standard format for 3D printing. The file may be obtained by contacting either of the first two authors of this paper. Each site should manufacture their own markers. A permanent marker (e.g., a Sharpie) or paint/stain should be used to improve contrast for photography.

If 3D printing is not possible, surface markers should be made of tapered PVC (polyvinyl chloride) approximately 25 mm outside diameter thick-walled (approx. 2.5 mm wall thickness) common water pipe. It may be tapered using a lathe to approximate drawing in Fig.1.7. The PVC can be stained with dark paint or primer prior to installation in the model to improve contrast with your sand and lighting conditions. If PVC is not available, the markers should be made from plastic with specific gravity approximately 1.5 to mitigate potential for uplifting out of the liquefying sand (Fig. 1.8).

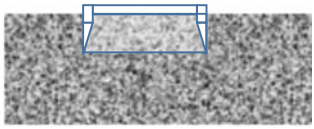

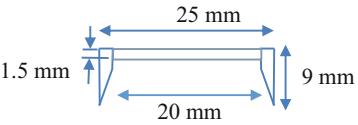

Surface_Marker_Larger_wCross.stl Previous Design (acceptable)

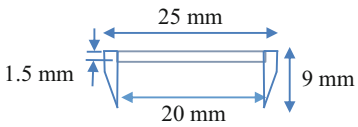

Surface_Marker_ImprovedDesign.stl Improved Design (Taper is reversed)

Fig. 1.7 Unstained 3D printed surface markers. Top right shows installation with 1.5 mm of marker above the soil surface. Dimensions are not critical but are recommended for consistency

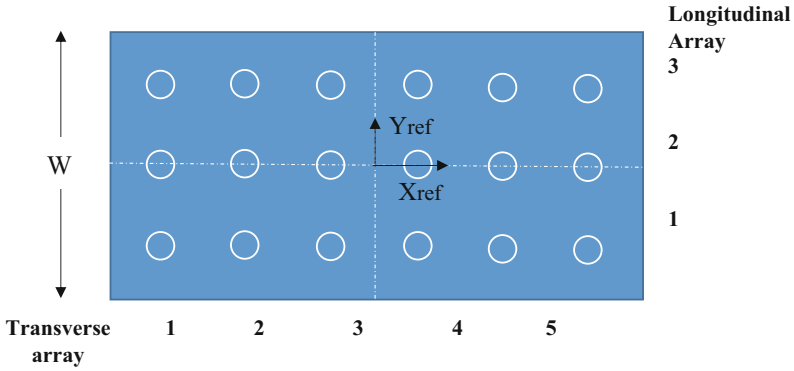

Fig. 1.8 Eighteen required surface markers at $X_{ref} = (-7.5, -3.5, -1.5, +1.5, +3.5, +7.5)$ m and $Y_{ref} = (0.3\ W, 0, -0.3\ W)$. Coordinate system was defined in Fig. 1.5 with the origin in the middle of the container, with $Z_{ref} = 0$ at the top surface of the base of the container

Lateral Displacements from Cameras Mounted on the Centrifuge

Cameras (preferably high speed) should be mounted to measure the plan view lateral displacements of surface markers during spinning. Camera with good resolution of horizontal movement should be used. UCD is presently planning to use a thick rigid plastic cover plate on top of the specimen to prevent surface waves. Four GoPro

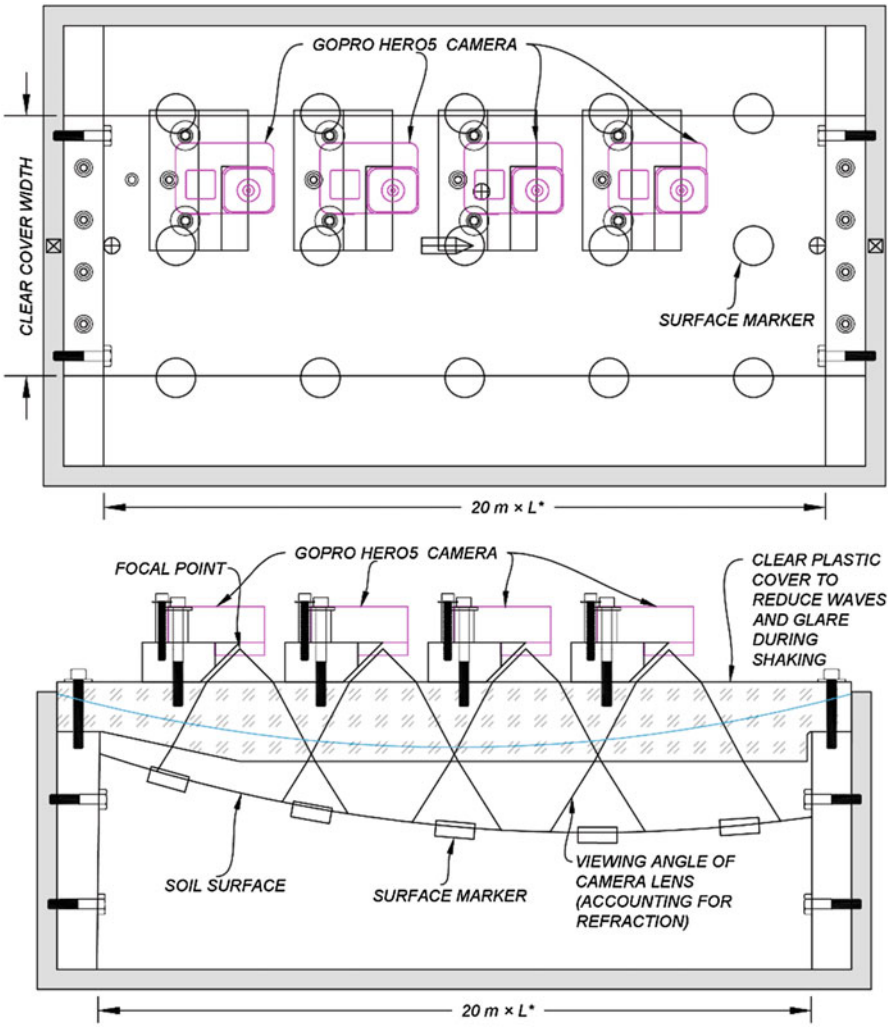

Fig. 1.9 UCD plan for cameras mounted on top of a thick plastic sheet to eliminate waves in images

cameras (running at 240 frames per second in 700p resolution) will be attached to the top of the cover plate to view different regions of the specimen (see Fig. 1.9). LED lights will also be attached to the plastic cover plate.

Residual Settlements from Pore Pressure Sensors

Residual pore pressures from pore pressure sensors will be used to determine the settlement of the pore pressure transducers before and after shaking. This requires

the sensors to be embedded in the soil (not attached to the model container) and very accurate recording data for a period of time after the pore water pressures are completely dissipated. Three main sources of error have been considered to make this strategy successful: (1) electronic noise, (2) incomplete pore pressure dissipation, and (3) drifting of the pore pressures due to residual tilting of the model container (perhaps due to sporadic overcoming of swing bearing friction during spinup and shaking) or due to changes in the water pressure associated with evaporation, changes in centrifuge g-level, or the degree of saturation.

1. The effect of electric noise on pore pressure sensor records can be dealt with by taking many data points over a period of time longer than the period of the noise. For example, if the noise is 50 or 60 Hz or higher, we could take the Residual Pore Pressure Average (RPPA) reading of data recorded at 2000 data points per second for a full second. This RPPA recording must be repeated before spinning the centrifuge, just before each shaking event, after complete dissipation of pore pressure from each shaking event, and after stopping the centrifuge.
2. As we are trying to resolve very small residual pore pressures to accurately measure residual settlements, it is crucial to ensure complete pore pressure dissipation. A good way to do this is to visually inspect the pore pressure record, find the time t_{99} required for pore pressures to drop to within 1% of the initial absolute pore pressure, and then wait ten times longer than t_{99} before recording the residual pore pressures. This might take about 10 min total between shaking events.
3. Sensors P9 and P10 accurately located in the bottom corner of the model containers should read the same RPPA increase during spinup from 1 g to the test acceleration, and ideally, they should return to the same RPPA after shaking and the same 1-g RPPA after stopping the centrifuge. Reasons for the difference between P9 and P10 include friction in the bucket hinge, the container base not being normal to the resultant g-vector, leakage or evaporation from the model container, or drifting of the centrifuge acceleration. Thus, the data from P9 to P10 sensors are crucial to allow us to compensate for small changes in g-level and water table elevation. Report RPM to an accuracy better than 0.5% before and after shaking. All of the RPPA values for all of the pore pressure sensors should be reported on one worksheet of the template.

Many facilities zeroed out the pore pressure sensors prior to each shaking event in LEAP-GWU-2015. This should not be done because it will defeat our effort to determine sensor settlements from residual pore pressures. If it is necessary to offset the electronic zero of the pore pressure sensors (e.g., for some electronic instrumentation limitation), RPPA values should be recorded before and after each electronic offset.

Direct Measurements of Sensor and Surface Marker Locations

The X, Y, and Z coordinates of the 15 surface markers shall be surveyed. Record the surface survey data in the spread sheet template showing the X, Y, and Z coordinates

of the top center of each marker. The required accuracy of the measurement is 1 mm for horizontal displacements and 0.5 mm for vertical settlements. The markers may be located using photogrammetric techniques, a laser scanner, or a depth gauge with a Vernier caliper that measures the locations relative to a rigid guide frame such as that pictured below. Suggested surface markers to facilitate analysis of lateral movements are specified in section (circular disks described above).

Colored Sand Layers, Noodles, and Sensor Locations During Dissection

Horizontal colored sand layers will be placed at the elevations of the central array of pore pressure sensors. The elevation of the sand relative to the model container reference coordinate system and relative to the pore pressure sensors should be measured before and after the tests.

Vertical markers will consist of spaghetti noodles placed vertically in the dry sand. The noodles should be placed in the sand after about half of the slope has been placed. An array of noodles along the window and along the longitudinal centerline should be placed before the test. The length of the noodles should be adjusted so they stick out about 1 or 2 mm above the ground surface before saturation. The deformed shape of the noodles should be exposed by excavation and photographed at the end of the shaking events.

Settlement Gage Sensors

Modified pore pressure transducers may be used to measure the surface settlement of the deposit (if possible at three locations along the surface). The concept of the modified pore pressure sensors is explained in Fig. 1.10. Traditional pore pressure transducers are sealed and connected through a flexible thin tubing to a constant head water reservoir. When the model is in equilibrium, the modified sensor reads the pressure imposed on it by the constant water head. As the soil settles during shaking and the sensor moves with it, the sensor reads an additional pressure that is directly proportional to the soil settlement. These modified were used in RPI test for LEAP-GWU-2015. Details of the sensors development are given in Antonaki et al. (2014). Additional details are given by Kokkali et al. (2018).

Tactile Pressure Sensors

Tactile pressure sensors may be attached to the container boundaries to measure the transient and residual soil pressure at the soil-container interface. Such sensors were used by RPI for LEAP-GWU-2015. The RPI group used tactile pressure sensors manufactured by Tekscan, Inc. (Cambridge, MA). The sensors need conditioning, equilibration, and calibration. Since the sensors are not waterproof, they were laminated, prepared for the specific soil-container interfaces, and then installed in

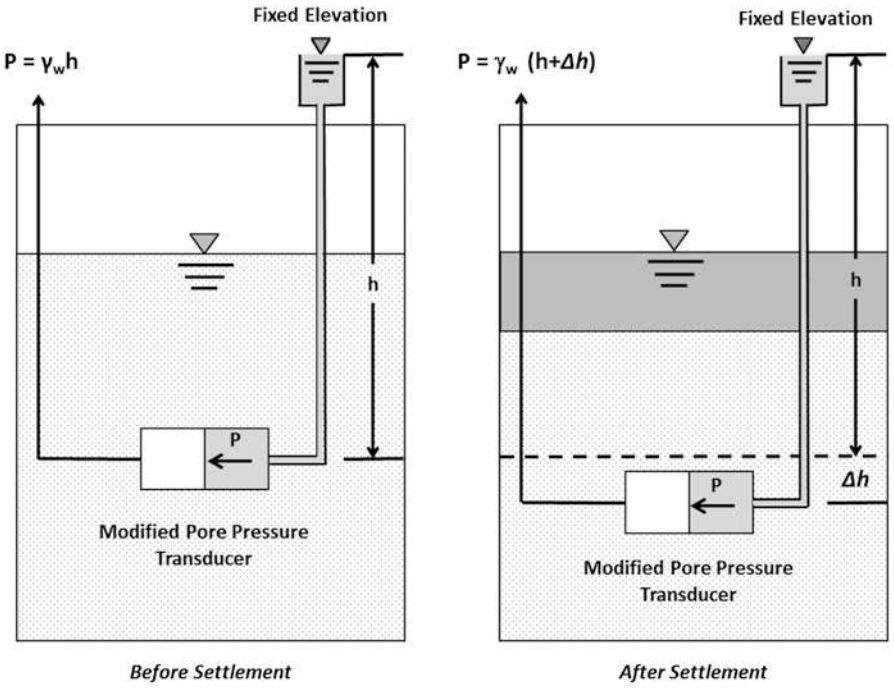

Fig. 1.10 Concept of the pressure transducer settlement gauges

the model container prior to the model construction (Figs. 3.3.1 and 3.3.2). The preparation procedure is described in detail in El Ganainy et al. (2014) and Kokkali et al. (2018).

1.5 Cone Penetration Testing

A new cone has been designed with a top load cell and no custom strain gauges at the cone tip as indicated in Fig. 1.11. The drawings are in a separate file in the shared box.com folder. Estimated cost for fabrication of this cone at UCD is approximately $1800 which includes a $500 load cell.

Cone penetration tests should be performed before and after every destructive ground motion. The rate of cone penetration, in model scale, should be scaled depending on the pore fluid viscosity in the model:

$$V_{\text{cpt, modelScale}} = (100\ \text{mm/s})/\mu^*$$

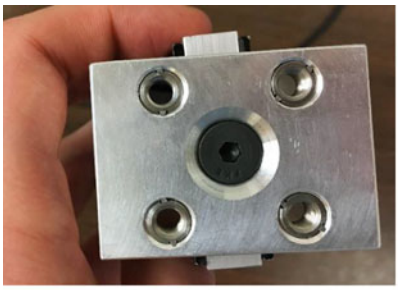

The spacing of the four M6x1mm bolts is 25.4 mm center to center in a square pattern.

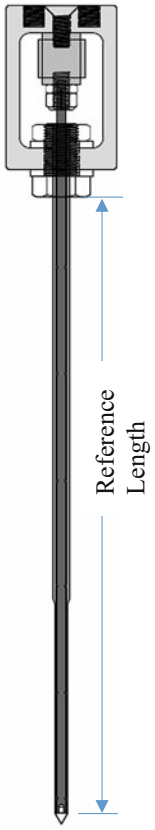

Cone		Ref. Length (mm) (not counting conical tip)
1	Ehime	124
2	Kwater	202
3	Kaist	202
4	Kyoto	194
5	NCU	294
6	NCU	294
7	Zhejiang	694
8	Zhejiang	644

Fig. 1.11 Images of a new design for LEAP-2017 CPT device and rod lengths of the devices used at different facilities

Thus if the test is done at 1/20 scale and $\mu^* = 20$, the velocity of penetration would be 5 mm/s, model scale. The data reported includes time, force, and actuator displacement in model units and qc vs depth below ground surface in prototype units. The tip resistance should be reported at depth intervals of 1 cm or less, prototype scale.

1.6 Shear Wave Velocity

Free bender elements, 12.7 mm × 8 mm in area as described by Brandenberg et al. (2006), could be used for measurement of shear wave velocity profiles. The methods used for interpretation of the data (see, for example methods described by Brandenberg et al. (2008), Lee and Santamarina (2005), and Montoya et al. (2012)) are to be determined by those doing the experiments. The sensors will be placed at mid-depth in the soil layer as indicated in Fig. 1.12 in a horizontal plane

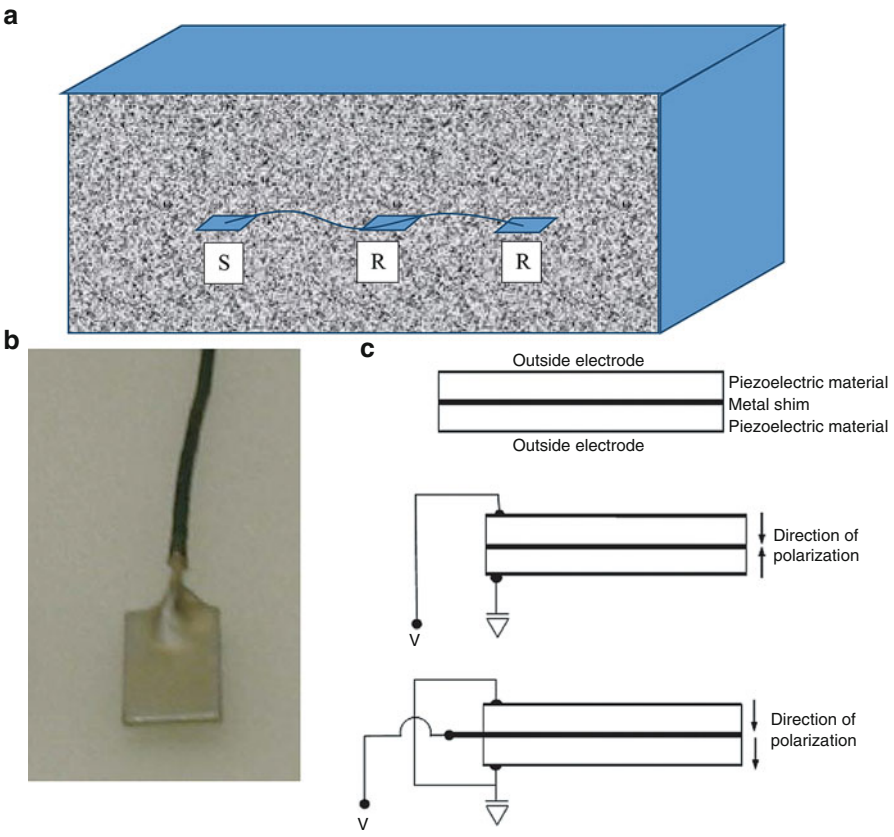

Fig. 1.12 (**a**) SV wave produced by source bender (S) and recorded by one or more receivers. (**b**) "Free" (not fixed to a block) bender element ready for embedment in soil. (**c**) Parallel and series wiring of benders (Brandenberg et al. 2006)

and measure vertically polarized horizontally travelling SV shear wave velocity. If capability is available, additional sensors may be placed at the quarter depths.

Shear wave velocity measurements should be made before and after every destructive shake. About half of the test sites are expected to retrieve shear wave velocity data in some LEAP-2017 experiments.

1.7 Ground Motions

1.7.1 Destructive Ground Motions

An excel worksheet that summarizes the target ground motions and the actual achieved ground motions posted in the Box.com folder and each site should refer

to the detailed test matrix to confirm specific assignments for their facility and promptly report the achieved input motions and densities as soon as possible after the experiment. The target motions in subsequent experiments may be adjusted based on achieved motions in previous experiments. The target motions are also summarized in Fig. 1.13.

For the first destructive motion, we will target a ramped sine wave very similar to that used for LEAP-GWU-2015. In that exercise we learned that many facilities shakers introduce high-frequency noise superimposed on the smooth ramped sine wave motion as shown, for example, in Figs. 1.14 and 1.15. Figure 1.16 shows that the velocity time series is much less affected by the high frequency that is so apparent in the acceleration time series of Fig. 1.14. Studies performed since LEAP-GWU-2015 indicate that the higher-frequency components have some but relatively less effect on the behavior of the model. To account for the reduced effect of high frequency, we have a working hypothesis that the effective PGA is

$$\mathrm{PGA}_{\mathrm{effective}} = \mathrm{PGA}_{1\mathrm{Hz}} + 0.5^{*}\mathrm{PGA}_{\mathrm{hf}} \tag{1.2}$$

where $\mathrm{PGA}_{\mathrm{hf}}$ represents the peak acceleration of the higher frequency components of the ground motion. The method of determining the $\mathrm{PGA}_{1\mathrm{Hz}}$ and $\mathrm{PGA}_{\mathrm{hf}}$ is described below and summarized in Fig. 1.15.

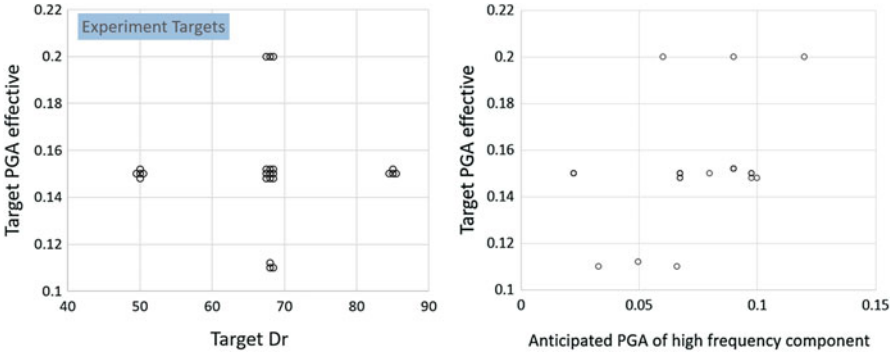

Fig. 1.13 Anticipated input motions for the experimental results

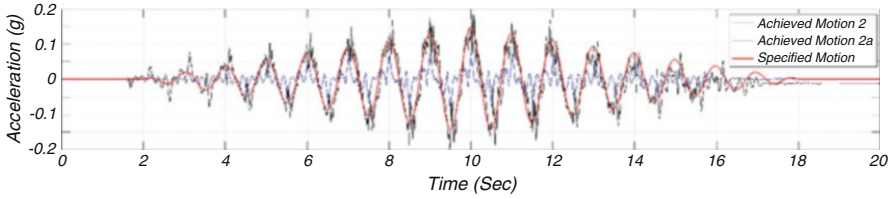

Fig. 1.14 Achieved and specified acceleration time history for Motions #2 and #2a of the ground motion sequence

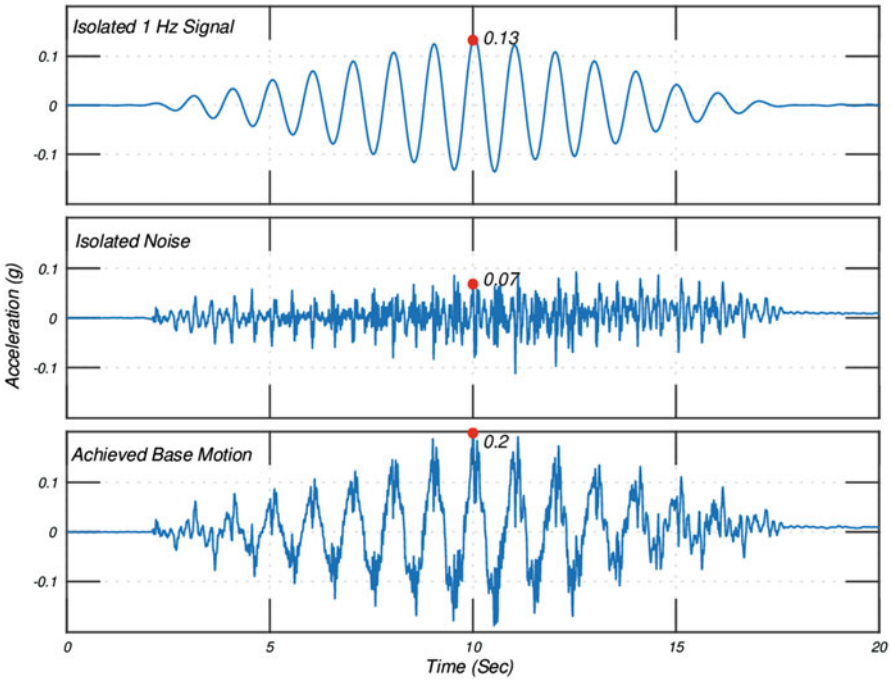

Fig. 1.15 Achieved base acceleration time history (bottom), high-frequency noise isolated from achieved signal (middle), and 1 Hz signal (top)

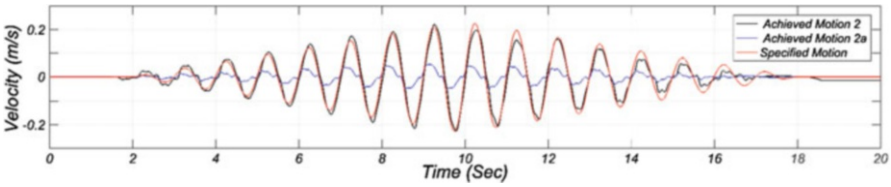

Fig. 1.16 Achieved and specified velocity time history for Motions #2 and #2a of the ground motion sequence

For the second destructive motion, pending additional discussion, discretion is given to the researchers at the test site. If, for example, the target for Destructive Motion #1 was missed in the first destructive motion, then Destructive Motion #2 would attempt to more accurately hit or to bracket the target. Another option for Destructive Motion #2 would be to attempt to impose the target motion for Destructive Motion #1 in a subsequent test for purposes of calibrating the shaking equipment. This would be a "practice" to enable more accurate performance in the subsequent test, and would also allow comparison of performance with different shaking histories. Other possibilities for Destructive Motion #2 are to try to mimic more realistic

ground motions, to intentionally introduce noise in the input motion to explore the validity of Eq. 1.2. Some researchers may also precisely repeat the first destructive motion to more rigorously evaluate the evolution of the behavior of the model due to the previous shaking event. Others may decide to vary the centrifuge acceleration, thereby increasing the prototype depth of the model, prior to the second destructive shaking event.

The experiment should be terminated before deformations are catastrophic because this will allow meaningful interpretation of post-test sensor location measurements, photographs of colored sand, surface marker locations, and spaghetti noodle markers.

However, if the deformations are very small after the second destructive motion, a third destructive motion may be applied at the discretion of the researcher. The third destructive motion should be the final ground motion. Possible options for the third motion are:

- Duplicate an achieved input motions of another LEAP site.
- Investigate effects of higher predominant frequency input motion.
- Investigate stress level effect by imposing higher/lower centrifuge g-level (different prototype layer thickness).
- Compare response in tapered sine to response in realistic earthquakes.

1.7.2 Nondestructive Ground Motions

The small amplitude 1 Hz motions used as nondestructive motions in the 2015 LEAP were found to be not very useful for characterizing the stiffness of the soils. It is possible that a high-frequency motion (with wavelengths comparable to the model thickness will be more useful). If $Vs = 200$ m/s and the wavelength is $\lambda = 4$ H (first mode resonance), the required frequency would be 12.5 Hz in prototype scale for the 4-m-deep deposit. It may be possible for the existing shakers to produce a very small vibration at this frequency Hz; if so, this could be useful for characterizing the soil between shakes. Caution must be exercised to avoid damaging or changing the state of stress of the model by shaking it too intensely. Banded white noise in the frequency range 6–20 Hz (or higher) prototype scale could be useful. RPI may use a Ricker wavelet to produce a short pulse containing these frequencies (RPI now in trials with practice test).

1.7.3 Assessment of Tapered Sine Wave (TSW) Ground Motions

The achieved base motion will be compared to the specified acceleration in a variety of ways as illustrated in Figs. 1.14, 1.15, and 1.16. The predominant frequency component of the motion (e.g., 1 Hz component for Motion #1) will be isolated by

use of a notched band pass filter with corner frequencies of approximately 0.9 and 1.1 times the predominant frequency. The predominant frequency component will be subtracted from the achieved motion in the time domain, producing a separate record of the high-frequency components as shown in Fig. 1.15 (middle). The record from UCD Motion#2 in LEAP-GWU-2015 was processed to produce the comparisons in Figs. 1.14, 1.15, and 1.16. The 0.2 g PGA of Motion #2, apparent in 14, has significant contributions from higher frequencies; the 1 Hz component of 0.13 g (Fig. 1.15) reasonably matches the specified 0.15 g for Motion #2. The achieved velocity obtained by integration of the acceleration record for Motion #2 follows that for the specified motion as illustrated in Fig. 1.16. A MATLAB script designed to process the signals (as shown in Fig. 1.14 to 1.16) has been posted for LEAP researchers in the Box.com folder.

1.8 Data Reporting Anticipated Plan/Concept

A specification for centrifuge test data will be detailed in a separate document; this will include templates for data submission and methods of uploading and sharing data.

1.8.1 New Leap Database

Results from LEAP-GWU-2015 were archived in a NEEShub Database. As part of this project, the database may be migrated to the new tools developed by the US NHERI DesignSafe Cyber Infrastructure Center. Experimenters should expect to fill out an excel workbook template for each model tested. The excel workbook data template will be similar to that used for LEAP-GWU-2015. In the meantime, we will share information using shared folders on box.com. Participating researchers should contact Bruce Kutter and Trevor Carey if they do not yet have access the LEAP-UCD-2017 Box.com files.

1.8.2 Dynamic Shaking Sensor Data

The dynamic sensor data must be recorded and reported at greater than 50 Hz prototype scale. Ideally, the data acquisition rate should be 200 samples per second (prototype time).

Acceleration data during shaking events should be reported in two formats: (1) as absolute acceleration without any baseline correction and (2) absolute acceleration

with baseline correction. Baseline correction parameters must be reported. A spreadsheet template will be provided.

1.8.3 Pore Pressure Long-Term Time Series Data

Residual pore pressure changes from before and after the earthquakes will be used as explained above to determine the residual settlement of the pore pressure transducers during the earthquakes. A separate tab in the spreadsheet workbook will be used to report the sensor data (at approximately one sample per second) obtained during the entire spin. Alternatively, Residual Pore Pressure Averages (RPPAs) will be recorded and reported at several stages of the experiment as described above.

1.8.4 Summary of Other Anticipated Report Requirements to Be Detailed in a Separate Document

A new template is under design for recording various items during model construction. It will likely involve another spreadsheet, with sections designed to take the following data.

- Sensor locations and marker locations.
- Description of the saturation process and documentation.
- Density calculations, photograph, and/or drawing of tools used to measure mass and volume of model.
- Quality control checks (grain size analysis and e_{max}, e_{min}).
- Description of any deviations from the specifications.
- Dimensions, mass, and part numbers of sensors.
- Description of how the model surface was curved.
- Photographic record of the top view of the surface markers at every stage of the test, and table of surface marker locations at various stages of the test.
- Photographic record of dissection and post-test sensor location measurement, and table showing locations of sensors, colored sand layers, and noodles before and after the testing.
- Results of inspection of the model and description of any special features of the deformed model surface, e.g., presence of sand boils, cracks at the boundaries, non-symmetric deformation, etc.
- Signal processing (analog filters, baseline correction, other corrections) to sensor data. If custom software is used, provide the software if possible.

Acknowledgments The experimental work on LEAP-UCD-2017 was supported by different funds depending mainly on the location of the work. The work by the US PIs (Manzari, Kutter, and Zeghal) is funded by National Science Foundation grants: CMMI 1635524, CMMI 1635307, and CMMI 1635040. The work at Ehime U. was supported by JSPS KAKENHI Grant Number 17H00846. The work at Kyoto U. was supported by JSPS KAKENHI Grant Numbers 26282103, 5420502, and 17H00846. The work at Kansai U. was supported by JSPS KAKENHI Grant Number 17H00846. The work at Zhejiang University was supported by the National Natural Science Foundation of China, Nos. 51578501 and 51778573; Zhejiang Provincial Natural Science Foundation of China, LR15E080001; and National Basic Research Program of China (973 Project), 2014CB047005. The work at KAIST was part of a project titled "Development of performance-based seismic design," funded by the Ministry of Oceans and Fisheries, Korea. The work at NCU was supported by MOST: 106-2628-E-008-004-MY3.

References

Antonaki, N., Sasanakul, I., Abdoun, T., Sanin, M. V., Puebla, H., & Ubilla, J. (2014). Centrifuge modeling of deposition and consolidation of fine-grained mine tailings. *Geo-Congress Technical Papers Geo-characterization and Modeling for Sustainability*, 3223–3232.

Brandenberg, S., Kutter, B., & Wilson, D. (2008). Fast stacking and phase corrections of shear wave signals in a noisy environment. *Journal of Geotechnical and Geoenvironmental Engineering, 134*(8), 1154–1165. https://doi.org/10.1061/(ASCE)1090-0241(2008)134:8(1154).

Brandenberg, S. J., Choi, S., Kutter, B. L., Wilson, D. W., & Santamarina, J. C. (2006). A bender element system for measuring shear wave velocities in centrifuge models. *Proceedings, 6th International Conference on Physical Modeling in Geotechnics, 1*, 165–170. https://nees.org/data/get/NEES-2006-0149/Documentation/References/Brandenberg_2006.pdf.

Carey, T. J., Kutter, B. L., Manzari, M. T., Zeghal, M., & Vasko, A. (2017). *LEAP soil properties and element test data*. https://doi.org/10.17603/DS2WC7W.

El Ganainy, H., Tessari, A., Abdoun, T., & Sasanakul, I. (2014). Tactile pressure sensors in centrifuge testing. *ASTM Geotechnical Testing Journal, 37*(1). https://doi.org/10.1520/GTJ20120061.

Garnier, J., Gaudin, C., Springman, S. M., Culligan, P. J., Goodings, D. J., Konig, D., Kutter, B. L., Phillips, R., Randolph, M. F., & Thorel, L. (2007). Catalogue of scaling laws and similitude questions in geotechnical centrifuge modelling. *International Journal of Physical Modelling in Geotechnics, 8*(3), 1–23.

Kokkali, P., Abdoun, T., & Zeghal, M. (2018). Physical modeling of soil liquefaction: Overview of LEAP Production Test 1 at Rensselaer Polytechnic Institute. *International Journal of Soil Dynamics and Earthquake Engineering, 113*, 629–649, https://doi.org/10.1016/j.soildyn.2017.01.036.

Kutter, B., Carey, T., Hashimoto, T., Zeghal, M., Abdoun, T., Kokalli, P., Madabhushi, G., Haigh, S., Hung, W.-Y., Lee, C.-J., Iai, S., Tobita, T., Zhou, Y. G., Chen, Y., & Manzari, M. T. (2017). LEAP-GWU-2015 experiment specifications, results, and comparisons. *International Journal of Soil Dynamics and Earthquake Engineering*. https://doi.org/10.1016/j.soildyn.2017.05.018.

Kutter, B. L. (2013). Effects of capillary number, bond number, and gas solubility on water saturation of sand specimens. *Canadian Geotechnical Journal, 50*(2), 133–144.

Lade, P. V., Liggio, C. D., & Yamamuro, J. A. (1998). Effects of non-plastic fines on minimum and maximum void ratios of sand. *Geotechnical Testing Journal*, 21(4), 336.

Lee, J. S., & Santamarina, J. C. (2005). Bender elements: Performance and signal interpretation. *Journal of Geotechnical and Geoenvironmental Engineering, 131*(9), 1063–1070.

Montoya, B. M., Gerhard, R., DeJong, J. T., Wilson, D. W., Weil, M. H., Martinez, B. C., & Pederson, L. (2012). Fabrication, operation, and health monitoring of bender elements for

aggressive environments. *Geotechnical Testing Journal, 35*(5), 1–15. https://doi.org/10.1520/GTJ103300. ISSN 0149-6115.

Okamura, M., & Inoue, T. (2012). Preparation of fully saturated models for liquefaction study. *International Journal of Physical Modeling in Geotechnics, 12*(1), 39–46. https://doi.org/10.1680/ijpmg.2012.12.1.39.